

Article

# Orthotropic Tension Behavior of Two Typical Chinese Plantation Woods at Wide Relative Humidity Range

Bingbin Kuai <sup>1</sup>, Xuan Wang <sup>1</sup>, Chao Lv <sup>1</sup>, Kang Xu <sup>2</sup>, Yaoli Zhang <sup>1</sup> and Tianyi Zhan <sup>1,\*</sup>

<sup>1</sup> College of Materials Science and Engineering, Nanjing Forestry University, Nanjing 210037, China; bbkuai@njfu.edu.cn (B.K.); wangxuan9210@outlook.com (X.W.); lvchao@njfu.edu.cn (C.L.); zhangyaoli@126.com (Y.Z.)

<sup>2</sup> Hunan Provincial Collaborative Innovation Center for High-Efficiency Utilization of Wood and Bamboo Resources, Central South University of Forestry and Technology, Changsha 410004, China; xkang86@126.com

\* Correspondence: tyzhan@njfu.edu.cn; Tel.: +86-025-85427058

Received: 2 June 2019; Accepted: 18 June 2019; Published: 19 June 2019



**Abstract:** *Research Highlights:* Orthotropic tension behaviors of poplar and Chinese fir were investigated at a wide relative humidity (RH) range. *Background and Objectives:* Poplar and Chinese fir are typical plantation tree species in China. Mechanical properties of plantation-grown wood varies from naturally-grown one. To utilize poplar and Chinese fir woods efficiently, fully understanding their moisture content (MC) and orthotropic dependency on tension abilities is necessary. *Materials and Methods:* Plantation poplar and Chinese fir wood specimens were prepared and conditioned in series RH levels (0–100%). Tensile modulus ( $E$ ) and strength ( $\sigma$ ) were tested in longitudinal ( $L$ ), radial ( $R$ ), and tangential ( $T$ ) directions. *Results:* The  $E$  and  $\sigma$  results in transverse directions confirmed the general influence of the MC that decreased with increasing MC. However, both  $E$  and  $\sigma$  in  $L$  direction showed a trend that increased at first, and then decreased when MC increased. The local maximums of stiffness and strength may be associated with straightened non-crystalline cellulose, induced by the penetration of water into the wood cell wall. Using the visualization method for compliance, the tension abilities of poplar and Chinese fir exhibited clear moisture and orthotropic dependency. *Conclusion:* Both poplar and Chinese fir showed a significantly higher degree of anisotropy in the  $L$ ,  $R$ , and  $T$  directions. The results in this study provided first-hand data for wooden construction and wood drying.

**Keywords:** orthotropic; tensile modulus; tensile strength; moisture content; relative humidity

## 1. Introduction

Wood supply gradually shifts from natural forest to plantation forest, with the worldwide trend toward intensive forest management to meet the wood demand and to protect the environment [1]. China serves as a typical example of this change, and China has planted more than 4 million hectares of new forest each year since the 1990s [2]. Poplar (*Populus spp.*) and Chinese fir (*Cunninghamia lanceolata* [Lamb.] Hook.) are common plantation species in China. Considerable differences in physical and mechanical properties can be found between naturally-grown (NG) and plantation-grown (PG) woods [3–5].

The properties of wood from plantation trees are inferior to those from natural forests, primarily because the proportion of juvenile part increases as rotation age is reduced [6]. It is widely accepted that density is the most important parameter in determining the mechanical properties of wood [7–11]. Due to the fast-grown characteristics of plantation wood, especially its juvenile wood, the density of PG wood is lower than NG wood [1]. Besides density, the inferior properties of PG wood are also influenced by its anatomical structures and chemical compositions. PG wood has shorter fibers with

considerably thinner cell walls. Compared to NG wood, PG wood has larger micro-fibril angles and the tendency for larger amounts of reaction wood in predominantly juvenile parts [12,13]. Large fibril angles, short fibers with thin walls, and low percentages of latewood in the annual ring all contribute to unsatisfactory strength and stiffness in PG wood [6].

Since wood by nature is anisotropic, it is usually described as a symmetric orthotropic material with three principal axes (longitudinal  $L$ , radial  $R$ , and tangential  $T$ ). Mechanical properties in  $L$ ,  $R$ , and  $T$  directions vary significantly. The mechanical characterization of wood, based on a three-dimensional approach, is needed as input for ambitious calculations in such fields like civil engineering and material science [14]. When used as truss or grille in a wooden construction, tension behavior in  $L$  direction is of importance, which has been published for numerous wood species [15–20]. Compared to the  $L$  direction, the tension behavior in  $R$  and  $T$  directions is limited to a few references. In mortise-tenon joint or glue joint area, wood and its composites would be loaded with transverse tensile force. During wood drying, when drying stress exceeds the ultimate tensile strength in transverse direction, crack, or split occur [21]. Hence, tension behavior in transverse direction also deserves to be investigated.

Wood moisture content (MC) influences nearly all its mechanical properties. The effect of MC on the mechanical properties of wood has been an extensively researched topic over the last decades [7,22–28]. In addition, the moisture-dependent orthotropic characteristics of some selected wood species have been published in Keunecke et al. [29], Hering et al. [14], Clauss et al. [30], Bachtiar et al. [31], and Jiang et al. [32]. With the exception of Poisson's ratios, stiffness and strength decrease with increasing MC [14,32], and the influence degree of MC on stiffness/strength in different directions are various. In addition, the decreasing stiffness or strength as a function of MC is observed at given MC ranges in the above mentioned reports.

Wood MC significantly varies at relative humidity (RH) ranges, from 0 to 100%. Fully understanding the MC-dependent mechanical properties at a wide RH range is necessary for utilizing wood and its composites efficiently. To obtain first-hand data of tension behavior of typical Chinese PG woods—poplar and Chinese fir, and to elucidate the orthotropic tensile behavior at wide relative humidity range, the tensile modulus and strength were investigated in RH range from 0 to 100%. The influences of MC on the elastic and strength were studied, and the moisture dependent stiffness was visualized in wide RH range as well.

## 2. Materials and Methods

### 2.1. Materials

Poplar (*Populus tomentosa* Carrière) and Chinese fir (*Cunninghamia lanceolata* [Lamb.] Hook.), two typical Chinese plantation resources, were selected as testing species. Poplar and Chinese fir were taken from Henan, and Zhejiang provinces, China, respectively. For each wood species, at least ten logs were cut. Once cut, the logs were air-dried for more than six months to a stable MC around 10 to 12%. The air-dried density of poplar and Chinese fir was  $0.50 \pm 0.04 \text{ g/cm}^3$ , and  $0.37 \pm 0.02 \text{ g/cm}^3$ , respectively. After air-dried, specimens without any visual defects were prepared with dimensions of  $370 \times 20 \times 15$  ( $L \times R \times T$ ),  $30 \times 150 \times 20$  ( $L \times R \times T$ ), and  $30 \times 20 \times 150$  ( $L \times R \times T$ ). Tensile tests were conducted along length direction of the specimens, hence, the three dimensions of specimens were named as  $L$ ,  $R$ , and  $T$ , respectively. All the specimens were processed as dog-bone shapes (Figure S1) according to Chinese national standards (GB/T 1938-2009 and GB/T 14107-2009).

A total number of 480 specimens were prepared and divided into eight groups with 20 specimens per load axes  $L$ ,  $R$  and  $T$ . Each group was conditioned in sealed containers over  $\text{P}_2\text{O}_5$ , or saturated solutions ( $\text{LiCl}_2$ ,  $\text{MgCl}_2$ ,  $\text{NaBr}$ ,  $\text{NaCl}$ ,  $\text{KCl}$ , and  $\text{KNO}_3$ ) or distilled water, which provided RH of 0, 11, 33, 58, 75, 85, 94 or 100% at room temperature (25 °C).

## 2.2. Tensile Test

After the conditioned period, the tensile test was performed using a Zwick Z100 universal testing machine with a 100 kN load cell. A displacement-controlled test was performed with a testing speed of about 1mm/min.

Tensile modulus ( $E$ , GPa) was obtained from the ratio of the stress ( $\sigma$ , N) to the corresponding strain ( $\varepsilon$ , mm<sup>2</sup>) in the linear elastic range:

$$E = \frac{\Delta\sigma}{\Delta\varepsilon} = \frac{\sigma_2 - \sigma_1}{\varepsilon_1 - \varepsilon_2} \quad (1)$$

where the subscripts “0” and “1” designate the corresponding data at 30 and 70% of the actual force of 50% elastic limit. The orientation and moisture-dependent elastic limits for poplar and Chinese fir were determined in the preliminary tests. To measure the tensile strength (ultimate stress)  $\sigma$ , the specimens were loaded with a constant loading rate to make sure the specimen failure was reached in  $90 \pm 30$ s.  $\sigma$  was tested using the following relationship

$$\sigma = \frac{P_{\max}}{A} \quad (2)$$

where  $P_{\max}$  is the maximum load at the failure point (N), and  $A$  is the cross section area at 1/2 length of the unloaded specimen (mm<sup>2</sup>). For  $L$ ,  $R$  and  $T$  specimens, the value of  $A$  is 60, 36, and 36 mm<sup>2</sup>, respectively.

## 2.3. Determination of Moisture Content (MC)

MC was determined by the mass of the specimens after conditioned at target RH ( $m_i$ ) and oven-dry ( $m_0$ ) on a dry basis:

$$MC = \frac{m_i - m_0}{m_0} \quad (3)$$

## 2.4. Statistical Analysis

The statistical software, SPSS version 17.0 (SPSS Inc, Chicago, IL, USA) was used for data analysis. Significant effects of MC on orthotropic modulus and strengths were analyzed by Duncan’s multiple comparison test ( $p = 0.05$ ).

# 3. Results and Discussion

## 3.1. Moisture Content

MCs of poplar and Chinese fir wood, at different RHs, are shown in Figure 1a,b. At each RH level, the average value of MC was calculated, based on the results of  $L$ ,  $R$ , and  $T$  specimens. Non-significant differences was found among specimens in three directions, regardless of RH levels. At a given RH level, the MC of Chinese fir was higher than poplar. Statistical analyses was conducted, as shown in Table S1. Both poplar and Chinese fir did not reached the fiber saturation point even at the most RH level. Wood MC was influenced by chemical components in cell wall, and associated with bulk density of wood. The lower density of Chinese fir delivered much more specific surface area and void in cell wall. Consequently, Chinese fir absorbed much moisture than poplar, especially at high RH levels.

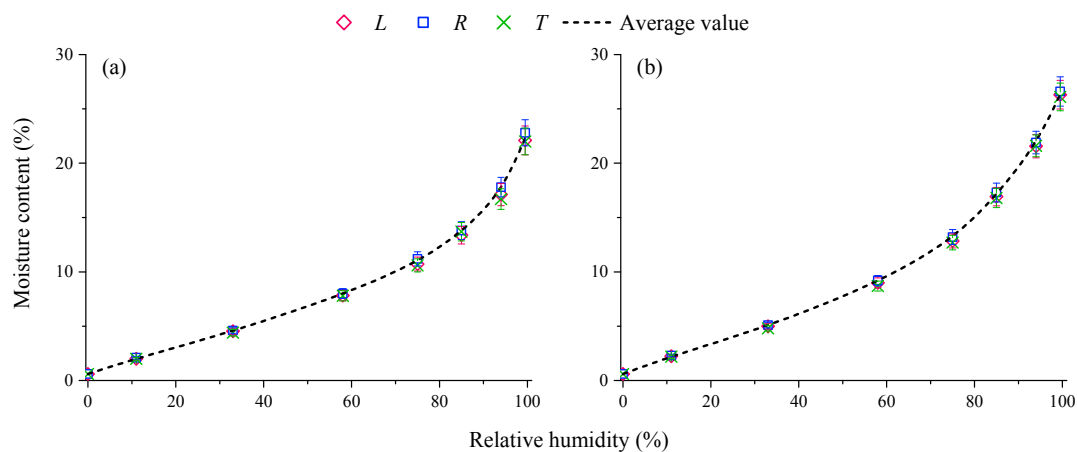


**Figure 1.** Moisture contents of poplar (a) and Chinese fir (b) at a series of relative humidity.

### 3.2. Moisture-Dependent Orthotropic Elasticity

#### 3.2.1. Tensile Modulus $E$

Changes of  $E$ , at different RH levels, are shown in Figure 2a,b, for poplar, and Chinese fir, respectively.  $E$  or  $L$  specimens was significantly greater than  $R$  or  $T$  specimens for both poplar and Chinese fir. The orientations of tracheids (in Chinese fir) or wood fiber (in poplar) in the  $L$  direction provided higher stiffness for  $L$  specimens than  $R$  or  $T$ . The stiffness of  $R$  specimens was higher than  $T$  for both poplar and Chinese fir. Anisotropic behavior, within the transverse plane, was evaluated by the value of  $E_R:E_T$ , while the MC-dependent  $E_R:E_T$  was still controversial. Decreased trend of  $E_R:E_T$  with increasing MC was concluded in Bachtiar [31], while Ozyhar et al. [33,34] and Jiang et al. [32] reported that  $E_R:E_T$  remained unchanged. In this study,  $E_R:E_T$  of poplar and Chinese fir increased from 1.33 to 1.56, and 1.18 to 1.45, respectively within the whole RH region (0–100%). Regardless of RH level, a higher value of  $E_R:E_T$  could be found for poplar than Chinese fir. Anatomical structure of poplar is more heterogeneous than that of Chinese fir, which was mainly consisted by tracheids. More cell types and arrangements donated much anisotropic behavior in the transverse plane of poplar.

Based on RH-dependent MC (Figure 1a,b) and  $E$  (Figure 2a,b), the relations between MC and  $E$  could be established. In Figure 2c,d, changes of  $E$  as a function of MC are displayed. Within the whole MC range,  $E_L$  increased first and then decreased. The local maximum value of  $E_L$  was 10.7, and 8.4 GPa, respectively for poplar at 2.0% MC and Chinese fir at 2.4% MC. The similar phenomena were also reported when wood was subjected to bending force by Takahashi et al. [35], Lu et al. [36], and Jiang et al. [37]. When water molecules penetrated into the wood cell wall, a slight amount of water induced a bridge effect involving hydrogen bonds forming a relative ordered cohesion state between molecular chains [35]. In the previous studies [14,30,32,38], the moisture ranges were limited, in hence, no local maximum value of  $E_L$  were reported.

Different from  $E_L$ , modulus in transverse directions ( $E_R$  and  $E_T$ ) decreased monotonically with increasing MC. Water acted as a softener for the wood polymers. Almost all the mechanical properties of wood were affected by moisture [39]. The plasticization of the amorphous polymers enhanced the flexibility of the polymer network when MC increased. A greater decrease in the extent of  $E$  of transverse specimens ( $R$  and  $T$ ) could be found than  $L$  specimens (Table S2). When MC increased from 0 to 26.3%, the decreasing rate of  $E_L$ ,  $E_R$ , and  $E_T$  was 36.5, 50.8, and 60.0%, respectively for Chinese fir. The matrix of lignin and hemicelluloses was much more sensitive to moisture than cellulose fibrils [40,41], and the matrix played a more important role than cellulose fibrils in the interpretation of transverse mechanical properties [42]. Hence, a greater decrease in the stiffness in the transverse direction could be found.

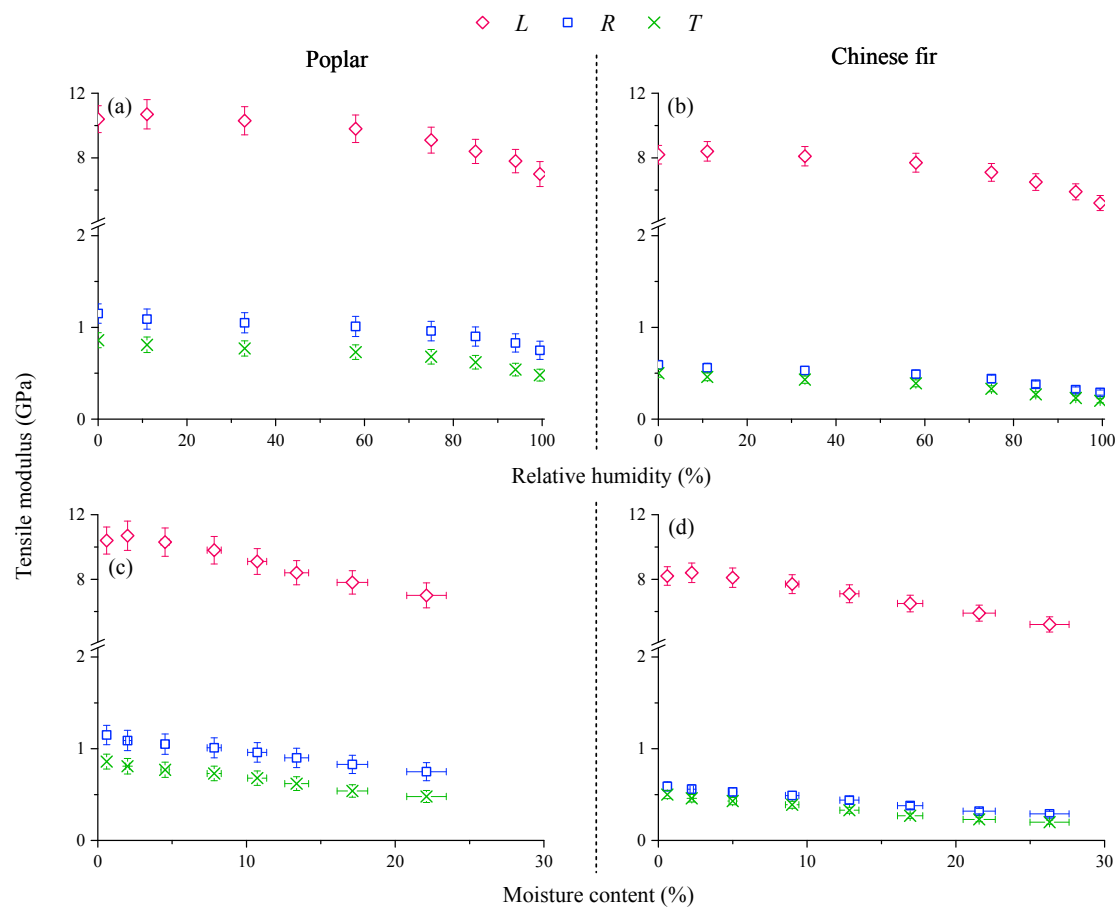


**Figure 2.** Influence of relative humidity on tensile modulus of poplar (a) and Chinese fir (b) and moisture dependence relations (c,d).

### 3.2.2. Visualization of the Orthotropic Elasticity

Elasticity at three orthotropic directions ( $L$ ,  $R$  and  $T$ ) could also be used to evaluate the elastic response when stress and strain deviated from these axes. Grimsel [43] proposed a first-time spatial illustration as “deformation body” and described the detailed transformation procedures. To demonstrate the moisture dependency of compliance, two-dimensional illustrations in the principle planes ( $L$ ,  $R$  and  $T$ ) of poplar and Chinese fir are presented, based on stiffness values ( $E_L$ ,  $E_R$ , and  $E_T$ ) (Figure 2a,b), and values of poisson ratio and shear modulus investigated by Bao et al. [1] and Cheng [44]. In Figure 3a,b, the relationships between compliance value and RH level were clearly visible. For both poplar and Chinese fir, increases in compliance as a function of increasing RH level can be observed in axis and off-axis directions. Moreover, the moisture-dependent compliance is spatially illustrated in Figure 4a,b by comparing the hemi deformation bodies at four RH levels. The deformation body can be interpreted as follows [29]: To any arbitrarily chosen axis in the three-dimensional coordinate system, representing the  $L$ ,  $R$ , and  $T$  directions of a wood species, an identical tensile load was applied. The bodies illustrated the degree of deformation depending on the load direction. By the deformation bodies, the influence of the MC on the overall deformation capability of poplar and Chinese fir wood, at a wide humidity range can be summarized effectively. Keunecke et al. [29], Hering et al. [14], Ozyhar et al. [33], Clauss et al. [30], and Jiang et al. [32] presented that the deformation body was suitable to describe the degree of the deformation dependent on the load direction.

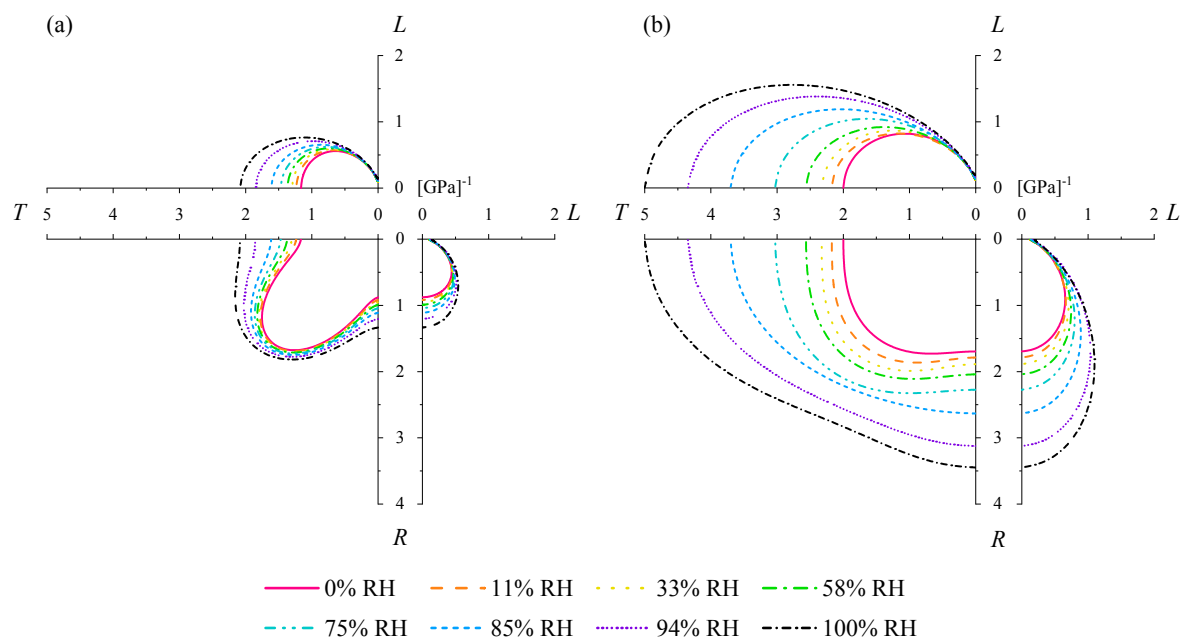


**Figure 3.** Load-directional dependence of poplar (a) and Chinese fir (b) wood compliance via polar diagrams for the principal planes of anisotropy.

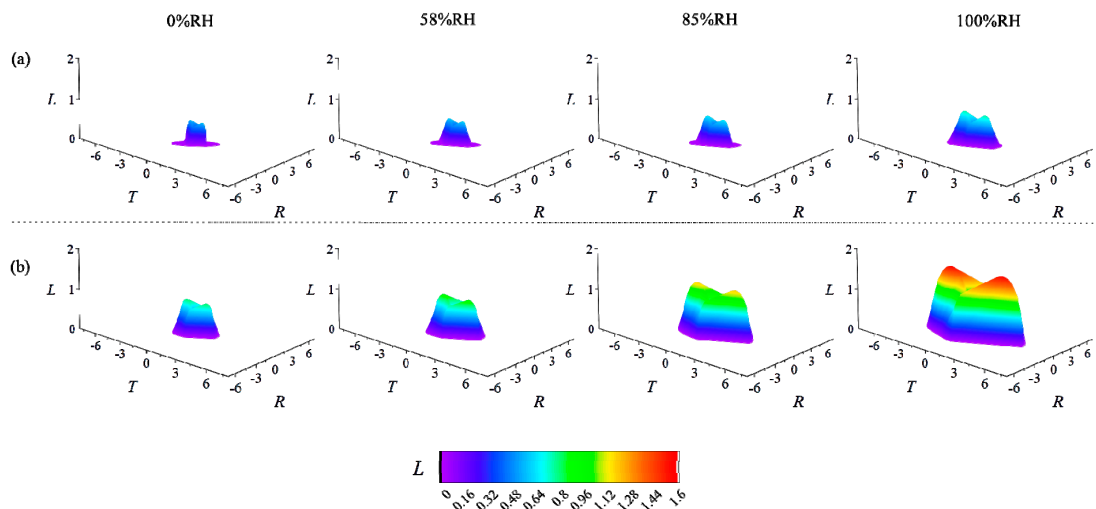


**Figure 4.** Load-directional dependence of poplar (a) and Chinese fir (b) wood compliance by the three-dimensional representation at four RH levels (0, 58, 85 and 100%).

### 3.3. Moisture-Dependent Orthotropic Strength

Figure 5a,b exhibit the changes of orthotropic  $\sigma$  at a series of RHs. Furthermore, the relationships of  $\sigma$  and MC are displayed in Figure 5c,d. At a given RH level (or MC),  $\sigma$  in the longitudinal direction ( $\sigma_L$ ) was significantly higher than in the transverse directions ( $\sigma_R$  and  $\sigma_T$ ) (Table S3). The theoretical tensile strength for cutting the main chains of cellulose molecular was about 8000 MPa, and the typical rupture was attributed to the shearing slip within the crystalline regions in  $L$  direction [45]. However, in  $R$  and  $T$  directions, the middle lamella was the most vulnerable area when resisting transverse tensile force. Within the transverse plane, the capacity of the bearing load in the  $R$  direction was superior than in the  $T$  direction. Taking 75% RH as an example, the value of  $\sigma_R:\sigma_T$  was 2.0:1, and 1.5:1, respectively for poplar and Chinese fir. This variation was associated with the orientation of wood ray cells. Wood ray played as reinforcement when tensile load applied in  $R$  direction [46]. According to Cheng [44], rays percentage of poplar and Chinese fir ranged 7–13, and 3–6 mm<sup>-1</sup>, respectively.

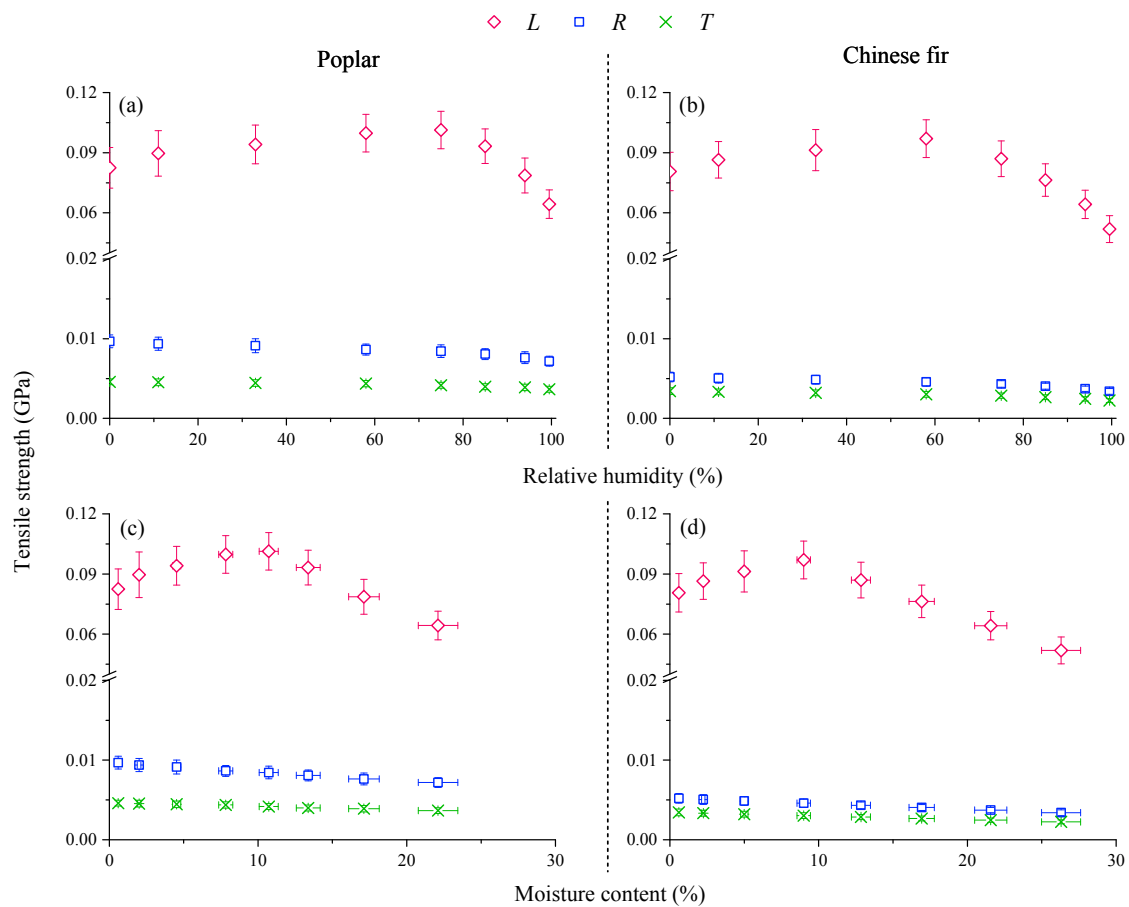


**Figure 5.** Influence of relative humidity on tensile strength of poplar (a) and Chinese fir (b) and moisture dependence relations (c,d).

Within the wide MC ranges, local maximum value of  $\sigma_L$  could be found (Figure 5c,d). For poplar and Chinese fir, the local maximum value of  $\sigma_L$  was 1.01 and 0.97 GPa at corresponding MC of 10.72 and 8.99%. Commonly, most of the mechanical properties of wood decreased with increasing MC, while the changing trend of  $\sigma_L$  within the wide MC ranges was different. In the wood cell wall, both crystalline and non-crystalline cellulose was embedded in a viscoelastic matrix [47]. Typically, slip and rupture in non-crystalline cellulose occurred prior to deformation of crystalline cellulose. When penetrated into the wood cell wall, water molecules induced the non-crystalline cellulose from curl states into straight states. The straightened non-crystalline cellulose may add the crystalline index of wood to some extent [48]. The increased crystalline index allowed more potential energy inside wood cell wall. Hence, local maximum value of  $\sigma_L$  can be found at certain MC condition. While, the molecule mechanism of the occurrence of the local maximum of  $\sigma_L$  deserves a depth investigation.

#### 4. Conclusions

The moisture-dependent orthotropic tension behavior (modulus and strength) of two typical Chinese plantation woods (poplar and Chinese fir) were qualified at wide humidity range (0–100 RH). Both poplar and Chinese fir showed significantly higher degrees of anisotropy in longitudinal (L), radial (R), and tangential (T) directions. The stiffness (E) and strength ( $\sigma$ ) results in transverse directions, and confirmed that E and  $\sigma$  decrease when MC increases. However, both E and  $\sigma$  in L direction showed a trend that increased at first, and then decreased when MC increased. The local maximums of stiffness and strength may be associated with the straightened non-crystalline cellulose induced by the penetration of water into the wood cell wall. Using the visualization method for compliance, tension

ability of poplar and Chinese fir exhibited clear moisture and orthotropic dependency. The results in this study provided first-hand data for wooden construction and wood drying.

**Supplementary Materials:** The following are available online at <http://www.mdpi.com/1999-4907/10/6/516/s1>, Figure S1: Schematic of *L* (a), *R* (b) or *T* (c) specimens, Table S1: Moisture content of poplar and Chinese fir, Table S2: Relative humidity-dependent stiffness of poplar and Chinese fir, Table S3: Relative humidity-dependent strength of poplar and Chinese fir.

**Author Contributions:** T.Z. conceived and designed the experiment. B.K., X.W., C.L., and K.X. performed the experiment and analyzed data. Y.Z. supervised the project. All the authors wrote the manuscript.

**Acknowledgments:** This research was financially supported by the National Key Research and Development Program of China (2017YFD0600202), the National Natural Science Foundation of China (No. 31700487), the Natural Science Foundation of Jiangsu Province (CN) (No. BK20170926).

**Conflicts of Interest:** The authors declare no conflict of interest.

## References

- Bao, F.; Jiang, Z.; Jiang, X.; Lu, X.; Luo, X.; Zhang, S. Differences in wood properties between juvenile wood and mature wood in 10 species grown in China. *Wood Sci. Technol.* **2001**, *35*, 363–375. [[CrossRef](#)]
- Xu, J. China's new forests aren't as green as they seem. *Nature News* **2011**, *477*, 371. [[CrossRef](#)] [[PubMed](#)]
- Phelps, J.; Chen, P. Lumber and wood properties of plantation-grown and naturally grown black walnut. *Forest Prod. J.* **1989**, *39*, 58–60.
- Bosman, M.T.; de Kort, I.; van Genderen, M.K.; Baas, P. Radial variation in wood properties of naturally and plantation grown light red meranti (*Shorea*, Dipterocarpaceae). *IAWA J.* **1994**, *15*, 111–120. [[CrossRef](#)]
- Bosman, M.T. Longitudinal variation in selected wood properties of naturally and plantation grown Light Red Meranti (*Shorea leprosula* and *S. parvifolia*, Dipterocarpaceae). *IAWA J.* **1996**, *17*, 5–14. [[CrossRef](#)]
- Bendtsen, B.; Senft, J. Mechanical and anatomical properties in individual growth rings of plantation-grown eastern cottonwood and loblolly pine. *Wood Fiber Sci.* **2007**, *18*, 23–38.
- Miyoshi, Y.; Kojiro, K.; Furuta, Y. Effects of density and anatomical feature on mechanical properties of various wood species in lateral tension. *J. Wood Sci.* **2018**, *64*, 509–514. [[CrossRef](#)]
- Niklas, K.J.; Spatz, H.C. Worldwide correlations of mechanical properties and green wood density. *Am. J. Bot.* **2010**, *97*, 1587–1594. [[CrossRef](#)]
- Kutnar, A.; Kamke, F.A.; Sernek, M. Density profile and morphology of viscoelastic thermal compressed wood. *Wood Sci. Technol.* **2009**, *43*, 57. [[CrossRef](#)]
- Liu, F.; Zhang, H.; Jiang, F.; Wang, X.; Guan, C. Variations in Orthotropic Elastic Constants of Green Chinese Larch from Pith to Sapwood. *Forests* **2019**, *10*, 456. [[CrossRef](#)]
- Emmerich, L.; Wülfing, G.; Brischke, C. The Impact of Anatomical Characteristics on the Structural Integrity of Wood. *Forests* **2019**, *10*, 199. [[CrossRef](#)]
- Cave, I.; Walker, J. Stiffness of wood in fast-grown plantation softwoods: The influence of microfibril angle. *Forest Prod. J.* **1994**, *44*, 43.
- Barnett, J.R.; Bonham, V.A. Cellulose microfibril angle in the cell wall of wood fibres. *Biol. Rev.* **2004**, *79*, 461–472. [[CrossRef](#)] [[PubMed](#)]
- Hering, S.; Keunecke, D.; Niemz, P. Moisture-dependent orthotropic elasticity of beech wood. *Wood Sci. Technol.* **2012**, *46*, 927–938. [[CrossRef](#)]
- Navi, P.; Rastogi, P.K.; Gresse, V.; Tolou, A. Micromechanics of wood subjected to axial tension. *Wood Sci. Technol.* **1995**, *29*, 411–429. [[CrossRef](#)]
- Kojima, Y.; Yamamoto, H. Properties of the cell wall constituents in relation to the longitudinal elasticity of wood. *Wood Sci. Technol.* **2004**, *37*, 427–434. [[CrossRef](#)]
- Hering, S.; Niemz, P. Moisture-dependent, viscoelastic creep of European beech wood in longitudinal direction. *Eur. J. Wood Wood Prod.* **2012**, *70*, 667–670. [[CrossRef](#)]
- Sonderegger, W.; Martienssen, A.; Nitsche, C.; Ozyhar, T.; Kaliske, M.; Niemz, P. Investigations on the physical and mechanical behaviour of sycamore maple (*Acer pseudoplatanus* L.). *Eur. J. Wood Wood Prod.* **2013**, *71*, 91–99. [[CrossRef](#)]
- Niemz, P.; Clauss, S.; Michel, F.; Hansch, D.; Hansel, A. Physical and mechanical properties of common ash (*Fraxinus excelsior* L.). *Wood Res.* **2014**, *59*, 671–682.

20. Oscarsson, J.; Olsson, A.; Enquist, B. Strain fields around knots in Norway spruce specimens exposed to tensile forces. *Wood Sci. Technol.* **2012**, *46*, 593–610. [[CrossRef](#)]
21. Wang, X.; Song, L.; Cheng, D.; Liang, X.; Xu, B. Effects of saturated steam pretreatment on the drying quality of moso bamboo culms. *Eur. J. Wood Wood Prod.* **2019**. [[CrossRef](#)]
22. Gerhards, C.C. Effect of moisture content and temperature on the mechanical properties of wood: An analysis of immediate effects. *Wood Fiber Sci.* **2007**, *14*, 4–36.
23. Rémond, R.; Passard, J.; Perré, P. The effect of temperature and moisture content on the mechanical behaviour of wood: A comprehensive model applied to drying and bending. *Eur. J. Mech A - Solids* **2007**, *26*, 558–572. [[CrossRef](#)]
24. Cave, I. Modelling moisture-related mechanical properties of wood Part I: Properties of the wood constituents. *Wood Sci. Technol.* **1978**, *12*, 75–86. [[CrossRef](#)]
25. Yu, Y.; Fei, B.; Wang, H.; Tian, G. Longitudinal mechanical properties of cell wall of Masson pine (*Pinus massoniana* Lamb) as related to moisture content: A nanoindentation study. *Holzforschung* **2011**, *65*, 121–126. [[CrossRef](#)]
26. Cave, I. Modelling moisture-related mechanical properties of wood Part II: Computation of properties of a model of wood and comparison with experimental data. *Wood Sci. Technol.* **1978**, *12*, 127–139. [[CrossRef](#)]
27. Ishimaru, Y.; Arai, K.; Mizutani, M.; Oshima, K.; Iida, I. Physical and mechanical properties of wood after moisture conditioning. *J. Wood Sci.* **2001**, *47*, 185–191. [[CrossRef](#)]
28. Cousins, W. Young's modulus of hemicellulose as related to moisture content. *Wood Sci. Technol.* **1978**, *12*, 161–167. [[CrossRef](#)]
29. Keunecke, D.; Hering, S.; Niemz, P. Three-dimensional elastic behaviour of common yew and Norway spruce. *Wood Sci. Technol.* **2008**, *42*, 633–647. [[CrossRef](#)]
30. Clauss, S.; Pescatore, C.; Niemz, P. Anisotropic elastic properties of common ash (*Fraxinus excelsior* L.). *Holzforschung* **2014**, *68*, 941–949. [[CrossRef](#)]
31. Bachtiar, E.V.; Sanabria, S.J.; Mittig, J.P.; Niemz, P. Moisture-dependent elastic characteristics of walnut and cherry wood by means of mechanical and ultrasonic test incorporating three different ultrasound data evaluation techniques. *Wood Sci. Technol.* **2017**, *51*, 47–67. [[CrossRef](#)]
32. Jiang, J.; Bachtiar, E.V.; Lu, J.; Niemz, P. Moisture-dependent orthotropic elasticity and strength properties of Chinese fir wood. *Eur. J. Wood Wood Prod.* **2017**, *75*, 927–938. [[CrossRef](#)]
33. Ozyhar, T.; Hering, S.; Niemz, P. Moisture-dependent elastic and strength anisotropy of European beech wood in tension. *J. Mater. Sci.* **2012**, *47*, 6141–6150. [[CrossRef](#)]
34. Ozyhar, T.; Hering, S.; Sanabria, S.J.; Niemz, P. Determining moisture-dependent elastic characteristics of beech wood by means of ultrasonic waves. *Wood Sci. Technol.* **2013**, *47*, 329–341. [[CrossRef](#)]
35. Takahashi, C.; Nakazawa, N.; Ishibashi, K.; Iida, I.; Furuta, Y.; Ishimaru, Y. Influence of variation in modulus of elasticity on creep of wood during changing process of moisture. *Holzforschung* **2006**, *60*, 445–449. [[CrossRef](#)]
36. Lu, J.; Jiang, J.; Wu, Y.; Li, X.; Cai, Z. Effect of moisture sorption state on vibrational properties of wood. *Forest Prod. J.* **2012**, *62*, 171–176. [[CrossRef](#)]
37. Jiang, J.; Lu, J.; Cai, Z. The vibrational properties of Chinese fir wood during moisture sorption process. *BioResources* **2012**, *7*, 3585–3596.
38. Kretschmann, D.E.; Green, D.W. Modeling moisture content-mechanical property relationships for clear southern pine. *Wood Fiber Sci.* **2007**, *28*, 320–337.
39. Salmén, L. Micromechanical understanding of the cell-wall structure. *C R Biol.* **2004**, *327*, 873–880. [[CrossRef](#)]
40. Englund, E.T.; Thygesen, L.G.; Svensson, S.; Hill, C.A. A critical discussion of the physics of wood–water interactions. *Wood Sci. Technol.* **2013**, *47*, 141–161. [[CrossRef](#)]
41. Kulasinski, K.; Guyer, R.; Derome, D.; Carmeliet, J. Water adsorption in wood microfibril-hemicellulose system: Role of the crystalline–amorphous interface. *Biomacromolecules* **2015**, *16*, 2972–2978. [[CrossRef](#)] [[PubMed](#)]
42. Åkerholm, M.; Salmén, L. The oriented structure of lignin and its viscoelastic properties studied by static and dynamic FT-IR spectroscopy. *Holzforschung* **2003**, *57*, 459–465. [[CrossRef](#)]
43. Grimsel, M. *Mechanisches Verhalten von Holz: Struktur-und Parameteridentifikation eines anisotropen Werkstoffes*; w.e.b.-Univ.-Verl.: Dresden, Germany, 1999; ISBN 3-933592-66-6.
44. Cheng, J. *Wood Science*; China Forestry Pub.: Beijing, China, 1985.

45. Bodig, J.; Jayne, B.A. *Mechanics of Wood and Wood Composites*; Van Nostrand Reinhold Company Inc.: New York, NY, USA, 1982.
46. Reiterer, A.; Burgert, I.; Sinn, G.; Tschegg, S. The radial reinforcement of the wood structure and its implication on mechanical and fracture mechanical properties—a comparison between two tree species. *J. Mater. Sci* **2002**, *37*, 935–940. [[CrossRef](#)]
47. Zhan, T.; Jiang, J.; Peng, H.; Lu, J. Dynamic viscoelastic properties of Chinese fir (*Cunninghamia lanceolata*) during moisture desorption processes. *Holzforschung* **2016**, *70*, 547–555. [[CrossRef](#)]
48. Ketoja, J.; Paavilainen, S.; McWhirter, J.L.; Róg, T.; Järvinen, J.; Vattulainen, I. Mechanical properties of cellulose nanofibrils determined through atomistic molecular dynamics simulations. *Nord. Pulp Pap. Res. J.* **2012**, *27*, 282–286. [[CrossRef](#)]



© 2019 by the authors. Licensee MDPI, Basel, Switzerland. This article is an open access article distributed under the terms and conditions of the Creative Commons Attribution (CC BY) license (<http://creativecommons.org/licenses/by/4.0/>).